

See discussions, stats, and author profiles for this publication at: <https://www.researchgate.net/publication/289518900>

# Contribution of trees and grasslands to the mitigation of human heat stress in a residential district of Freiburg...

Article in *Landscape and Planning* · January 2016

DOI: 10.1016/j.landurbplan.2015.12.004

CITATIONS

30

READS

539

3 authors:



**Hyunjung Lee**

Urban Climatology

11 PUBLICATIONS 134 CITATIONS

[SEE PROFILE](#)



**Helmut Mayer**

University of Freiburg

283 PUBLICATIONS 6,910 CITATIONS

[SEE PROFILE](#)



**Liang Chen**

East China Normal University

22 PUBLICATIONS 673 CITATIONS

[SEE PROFILE](#)

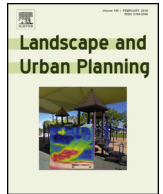
Some of the authors of this publication are also working on these related projects:



BUBBLE - Basel Urban Boundary Layer Experiment [View project](#)



Urban Thermal Environment under Climate Change [View project](#)



## Research Paper

# Contribution of trees and grasslands to the mitigation of human heat stress in a residential district of Freiburg, Southwest Germany



Hyunjung Lee<sup>a,\*</sup>, Helmut Mayer<sup>a</sup>, Liang Chen<sup>b</sup>

<sup>a</sup> Chair of Meteorology and Climatology, Albert-Ludwigs-University of Freiburg, Germany

<sup>b</sup> School of Geographic Sciences, East China Normal University, Shanghai, PR China

## HIGHLIGHTS

- Human heat stress in a residential district is simulated for different green coverage scenarios.
- The impact of trees on human thermal comfort is quantified for a heat wave day.
- Green coverage is capable of reducing mean radiant temperatures by 43 K.
- Green coverage is capable of reducing mean physiologically equivalent temperatures by 22 K.
- The human-biometeorological performance of the ENVI-met model is validated.

## ARTICLE INFO

## Article history:

Received 14 November 2014

Received in revised form 5 December 2015

Accepted 10 December 2015

## Keywords:

Human heat stress  
Green coverage changes  
Residential district  
ENVI-met simulations  
Model evaluation

## ABSTRACT

The potential of urban green coverage to mitigate human heat stress is studied using the ENVI met model V4. The simulation domain is a residential district in Freiburg, a mid-size city in Southwest Germany. It is characterised by residential buildings and street canyons with asphalt surfaces, grasslands and broad-leaved trees. The ENVI-met model was validated against human-biometeorological measurements and demonstrated good performance when simulating the urban thermal environment in terms of air temperature ( $T_a$ ) and human heat stress in terms of mean radiant temperature ( $T_{mrt}$ ) and physiologically equivalent temperature (PET). Simulations were performed for the heat wave day of 4 August 2003, which is a typical scenario for future summer weather in Central Europe as projected by climate models. Four scenarios with different types of green coverage were simulated. The results enable quantification of the daytime and nocturnal contributions of trees and grasslands, respectively, to the mitigation of human heat stress on different spatial scales. Averaged over 10–16 CET, trees on grasslands lead to a mitigation effect up to 2.7 K for  $T_a$ , 39.1 K for  $T_{mrt}$  and 17.4 K for PET. In comparison, the effect of grasslands can be up to 3.4 K for  $T_a$ , 7.5 K for  $T_{mrt}$  and 4.9 K for PET. Based on the findings, design implications are also provided from the perspective of urban human-biometeorology.

© 2015 Elsevier B.V. All rights reserved.

## 1. Introduction

Each city is embedded in a specific regional atmospheric situation, which is determined by its respective climate zone and current weather situation as well as topographic and land use conditions (Holst & Mayer, 2011). Within a city, the regional atmospheric situation is modified by urban structures, land covers and air-surface

energy exchange processes, which lead to different urban meteorological phenomena such as the well-known urban heat island effect (Kuttler, 2010).

The regional atmospheric situation is influenced by regional climate change. For Central Europe, results of climate simulations indicate that severe heat waves will be more frequent and intense, as well as longer lasting in the future (Beniston, 2013). On the other hand, the design of Central European cities is not adapted to severe heat, which causes negative impacts on the health and well-being of citizens (Hajat & Kosatky, 2010). The threat of heat stress is gradually increasing in many Central European cities due to demographic changes with raising proportions of elderly people (Federal Statistical Office of Germany, 2011). Senior citizens are particularly

\* Corresponding author.

E-mail addresses: [hyunjung.lee@meteo.uni-freiburg.de](mailto:hyunjung.lee@meteo.uni-freiburg.de) (H. Lee), [helmut.mayer@meteo.uni-freiburg.de](mailto:helmut.mayer@meteo.uni-freiburg.de) (H. Mayer), [lchen@des.ecnu.edu.cn](mailto:lchen@des.ecnu.edu.cn) (L. Chen).

vulnerable to heat stress as people's thermo-physiological capacity for adaptation to severe heat decreases with age (Laschewski & Jendritzky, 2002). With this background, urban design measures aimed at maintaining local human thermal comfort, even under severe heat stress, have recently drawn increasing attention (Lee & Mayer, 2013; Lee, Holst, & Mayer, 2013; Mayer, Holst, Dostal, Imbery, & Schindler, 2008; Moonen, Defraeye, Dorer, Blocken, & Carmeliet, 2012; Müller, Kuttler, & Barlag, 2014). With respect to improving the health and well-being of citizens, recommendations and implementation of design strategies need to be based on scientific findings from the urban human-biometeorological perspective.

The human perception of heat is governed by the local thermal environment and thermo-physiological processes, which are combined in the human heat budget (Höppe, 1999; Mayer, 1993). Therefore, human perception of the local thermal environment cannot be described only by the air temperature ( $T_a$ ), as it is also influenced by other meteorological variables such as the mean radiant temperature ( $T_{mrt}$ ), wind speed ( $v$ ) and water vapour pressure (VP). A number of thermal comfort assessment indices have been developed in the last 30 years based on the human heat budget (McGregor, 2011). These indices enable the evaluation of the thermal environment in a thermo-physiologically significant way. As such indices, like the physiologically equivalent temperature (PET) (Mayer & Höppe, 1987), were developed and successfully applied in urban settings (Acero & Herranz-Pascual, 2015; Chen & Ng, 2012; Holst & Mayer, 2011; Lee & Mayer, 2015; Lee, Mayer, & Schindler, 2014), they can be used to analyse the potential of urban greening for the mitigation of urban thermal environments and provide implications for urban design.

The cooling effect of street trees by shading and evapotranspiration has been emphasised and design recommendations have been proposed (Bowler, Buyung-Ali, Knight, & Pullin, 2010; Coutts, White, Tapper, Beringer, & Livesley, 2015; Klemm, Heusinkveld, Lenzholzer, & van Hove, 2015; Lee & Mayer, 2013, 2015; Mullaney, Lucke, & Trueman, 2015; Shahidan, Shariff, Jones, Salleh, & Abdullah, 2010; Shashua-Bar, Pearlmutter, & Erell, 2011). It has been found that urban greening contributes to a reduction in the heat input into all urban open spaces in the daytime. In combination with the local airflow, the magnitude of such cooling effects mainly determines whether the thermal load at night can be alleviated to a level where indoor air conditioning systems do not need to be used. However, so far most previous investigations on the cooling effect of urban greening are focused only on  $T_a$ . The human-biometeorological aspect of local mitigation of human heat stress has only been addressed in a few studies of individual sites (Acero & Herranz-Pascual, 2015; Chen & Ng, 2013; Cohen, Potchter, & Matzarakis, 2012; Coutts et al., 2015; Holst & Mayer, 2011; Lee & Mayer, 2015; Lee et al., 2013; Mayer, Kuppe, Holst, Imbery, & Matzarakis, 2009; Shashua-Bar et al., 2011).

Taking into account the increasing heat waves in Central Europe in the future, the objective of this study is to expand the existing knowledge of the potential of urban greening to mitigate human heat stress from the human-biometeorological perspective. A residential district in Freiburg (Southwest Germany) was selected for the case study. Human-biometeorological simulations using the ENVI-met model were conducted for a typical Central European heat wave day. With respect to urban human-biometeorology and applications in urban design, the study emphasises the following issues: (i) the current green land use in the study site, (ii) different green coverage scenarios in the study site, (iii) the local thermal environment in terms of  $T_a$ , (iv) human heat stress in terms of  $T_{mrt}$  and PET, (v) representative street canyons in the study site, and (vi) longer time periods that are more relevant to design strategies than a certain time slot in the afternoon.

## 2. Methods

### 2.1. Simulation day and study site

Numerical simulations using the ENVI-met model were conducted for 4 August 2003. It was a clear-sky summer day in the severe heat wave of 2003 in Central and Western Europe (Rebetez et al., 2006). It represents typical atmospheric conditions of future summer weather in Central Europe (Beniston, 2013). As this day was at the beginning of the heat wave, urban greening was not affected by the high air temperature and lack of water.

A residential district (Fig. 1) located in the northern downtown of Freiburg (44° 00' N, 7° 51' E, 280 m asl), a mid-size city (222,000 residents in 2014) in Southwest Germany, was selected as the study site. Arranged fairly evenly, it consists of three-storey residential buildings with pitched roofs and street canyons with asphalt surfaces, grasslands and broad-leaved trees (mainly maple trees). The aspect ratio (H/W) of the street canyons is approximately 0.5. According to the classification of the local climate zone scheme (Stewart & Oke, 2012), the study site can be characterised as a mixture of the built types LCZ 3 (compact low-rise) and LCZ 5 (open mid-rise).

### 2.2. Simulation model

The three-dimensional micro-meteorological model ENVI-met (Bruse & Fleer, 1998) is one of the few micro-scale models that meet the criteria for an accurate simulation of physical processes and resulting micro-meteorological phenomena within the urban canopy and boundary layer (Erell, Pearlmutter, Boneh, & Bar Kutiel, 2014; Huttner, 2012). ENVI-met is a three-dimensional Computational Fluid Dynamics (CFD) model that simulates surface-plant-air-interactions in urban environments. Its physical basis has been well explained in the literature (Ali-Toudert & Mayer, 2006; Bruse & Fleer, 1998; Huttner, 2012; Samaali, Courault, Bruse, Olioso, & Occelli, 2007; Taleghani, Kleerekoper, Tenpierik, & van den Dobbelsteen, 2015). Different versions of the ENVI-met model have been successfully applied in simulations of the micro-meteorological and human-biometeorological impacts of building and street design as well as urban greening (Acero & Herranz-Pascual, 2015; Ali-Toudert & Mayer, 2006, 2007; Chen & Ng, 2013; Lee & Mayer, 2015; Middel, Häb, Brazel, Martin, & Guhathakurta, 2014; Müller et al., 2014; Ng, Chen, Wang, & Yuan, 2012; Perini & Magliocco, 2014; Skelhorn, Lindley, & Levermore, 2014; Srivani & Hokao, 2013; Yang, Zhao, Bruse, & Meng, 2013).

In this study, the up-to-date ENVI-met model V4 (released in 2013) and its sub-module BioMet (v. 1.0) were used for the numerical simulations. The BioMet sub-module enables the calculation of PET according to the method described by Höppe (1999). The assignment of PET ranges corresponding to different human thermal sensation levels is based on the classification scheme (Table 1) derived by Holst and Mayer (2010) for hot summer conditions in Freiburg. In contrast to previous versions, version V4 has some essential improvements (Acero & Herranz-Pascual, 2015; Huttner, 2012; Yang et al., 2013) such as the implementation of a forcing function. This means that 1-h values of  $T_a$  and relative humidity (RH) measured at a meteorological station, which is adjacent to the simulation domain, can be included in the simulation. Therefore, more realistic simulation results can be achieved. In this study, 1-h  $T_a$  and RH data were taken from a meteorological station at the top of a high-rise building located at the upper border of the simulation domain, as shown in Fig. 1.

The investigation site allowed for validation of the human-biometeorological performance of the applied model in terms of  $T_a$ ,  $T_{mrt}$  and PET. It was based on field studies on human thermal comfort, which were simultaneously conducted at five

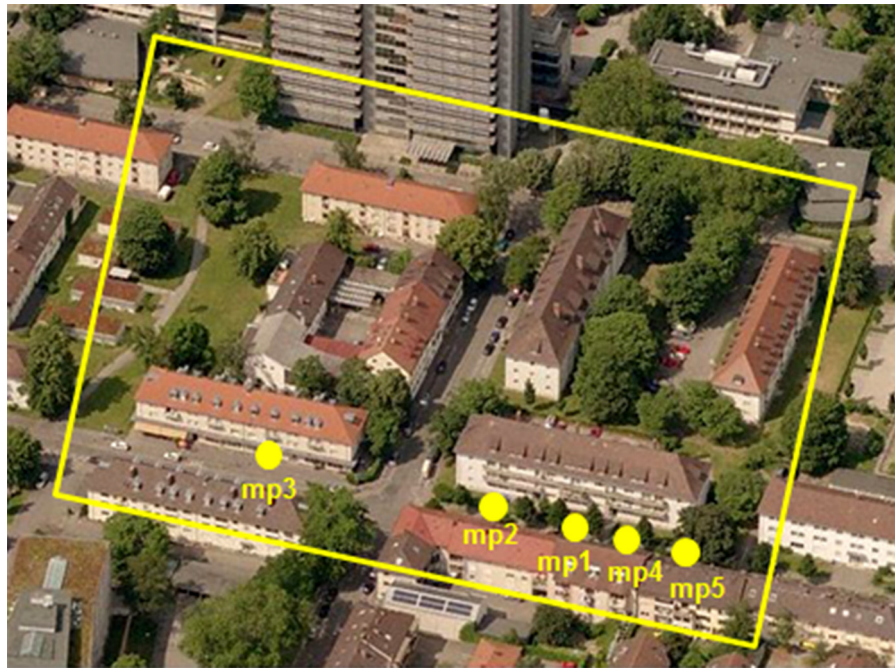


**Fig. 1.** Simulation domain in Freiburg (yellow outline) and locations of human-biometeorological measuring sites (mp1 to mp5) on 27 July 2009 (For interpretation of the references to colour in this figure legend, the reader is referred to the web version of this article.).

Source: Bing Maps, 2009

**Table 1**

Ranges of PET values for different warm levels of human thermal sensation according to the ASHRAE thermal sensation scale, derived from questionnaires and simultaneous human-biometeorological field studies in the summer of 2010 in Freiburg (Holst & Mayer, 2010).

ASHRAE thermal sensation scale		PET range (°C)
Name	Scale	
Slightly warm	+1	30–34
Warm	+2	35–40
Hot	+3	>40

measuring sites (mp1 to mp5) on 27 July 2009. The sites were located at the SSW-facing sidewalk of an ESE-WNW oriented street canyon with aspect ratio of 0.5 (Fig. 1) and had a heterogeneous urban micro-environment. The day of 27 July 2009 was a typical clear-sky summer day in Central Europe. Tailor-made human-biometeorological measuring systems recorded meteorological parameters required to determine  $T_{mrt}$  and PET. The measurements were conducted at a height of 1.5 m agl (Mayer et al., 2008). Technical specifics of the equipment and methods are explained in detail by Holst and Mayer (2010, 2011) and Lee et al. (2013). In particular,  $T_{mrt}$  was determined by a state-of-the-art six-directional method to measure the short- and long-wave radiant flux densities from the three-dimensional environment of a human-biometeorological reference person (Lee et al., 2013; Mayer et al., 2008), while PET was calculated according to the approach described by Höppe (1999).

### 2.3. Setup for the numerical simulations

The simulation domain was subdivided into a 3-D grid. Its horizontal domain consisted of 150 by 150 grids of 1 m resolution. The vertical grid size was also 1 m, whereby the lowest vertical grid was divided into five equidistant sub-grids of 0.2 m (Huttner, 2012). The horizontal domain covered a total area of 2.25 ha. It was expanded by an additional space of 20 m at each border to consider the lateral boundary conditions. The meteorological data used in the

**Table 2**

Meteorological data for the configuration file of the ENVI-met model on both simulation days,  $v$ : wind speed,  $dd$ : wind direction,  $s$ : specific humidity,  $z_0$ : roughness length,  $\alpha$ : short-wave albedo,  $\varepsilon$ : long-wave emissivity.

Variables	27 July 2009	4 August 2003
$v$ (10 m agl)	1.0 m/s	
$dd$	270° (from West)	
$s$ (2500 m agl)	7.0 g/kg	10.6 g/kg
$z_0$ (at reference point)	0.1 m	
$\alpha$	Buildings: 0.30, asphalt surfaces: 0.20 Grasslands: 0.20, trees: 0.20	
$\varepsilon$	Buildings: 0.90, asphalt surfaces: 0.90 Grasslands: 0.95, trees: 0.95	

configuration file of the ENVI-met model for both simulation days (27 July 2009 and 4 August 2003) are summarised in Table 2. In contrast to previous versions of ENVI-met, values of the initial  $T_a$  and RH at a height of 2 m agl were provided by the forcing function. As the ENVI-met model had a high spatial resolution, accurate 3-D input data were necessary to take into account the actual specific building characteristics and tree dimensions. Therefore, height, crown length, maximum crown diameter, trunk diameter at breast height (DBH) and leaf area index (LAI) were determined for each of the 45 trees within the simulation domain using on-site measurements. The simulations for both days started at 5 CET and ran for a continuous period of 24 h.

### 2.4. Simulation scenarios

The current urban green pattern at the study site represents typical residential districts in Central European cities. To quantify the mitigating effect of the current green pattern on human heat stress on the heat wave day of 4 August 2003, and also the specific contributions of trees and grasslands, four different scenarios (Fig. 2) were simulated:

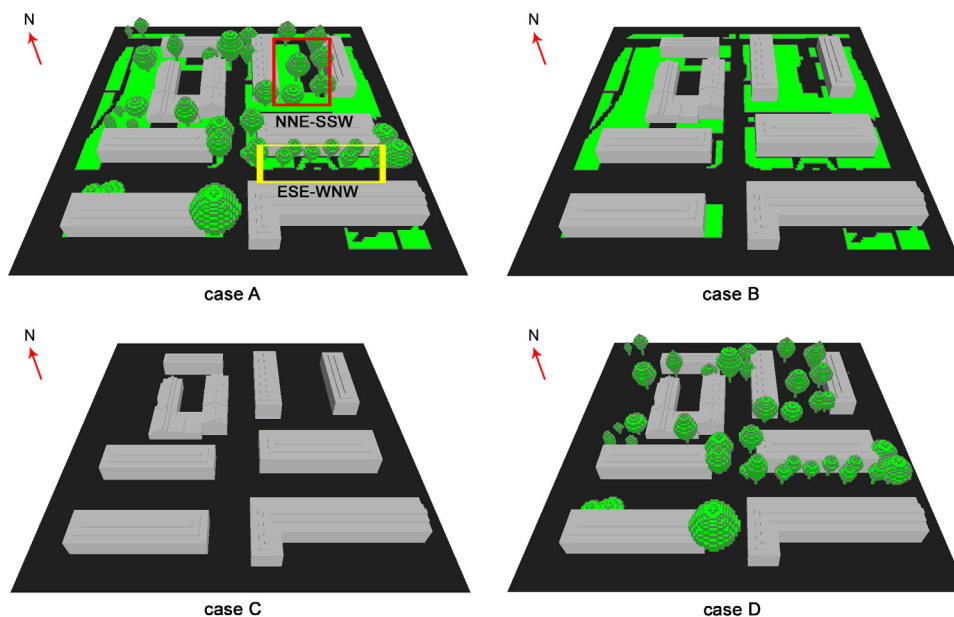


**Fig. 2.** Visualisation of the area input file for the ENVI-met simulations related to case A (current land use configuration), case B (case A without trees), case C (case B without any urban greening) and case D (case C including trees).

**Table 3**  
Partitioning of surface types in terms of their areas for different land use scenarios in the simulation domain (2.25 ha: 100%).

Land use situation	Scenarios			
	Case A	Case B	Case C	Case D
	Current land use configuration	Current land use configuration without all trees	Current land use configuration without trees and grasslands	Current land use configuration with asphalt surfaces instead of grasslands
Building surfaces	31%	31%	31%	31%
Asphalt surfaces	41%	41%	69%	69%
Grasslands	28%	28%	0%	0%
Overall cross sectional areas of the tree crowns	17%	0%	0%	17%

- case A: current land use situation including both trees and grasslands;
- case B: case A but excluding trees, i.e., only buildings, asphalt surfaces and grasslands remain;
- case C: case B but replacing all grasslands with asphalt surfaces, i.e., only buildings and asphalt surfaces remain;
- case D: case C but including trees.

With these four settings, the differences of  $T_a$ ,  $T_{mrt}$  and PET between cases C and A could reveal the total heat mitigation of the current urban green situation. The differences between cases B and A could indicate the effect of trees, while the differences between cases C and B could show the effect of grasslands. Last but not least, the differences between cases C and D could reveal the human-biometeorological effect of trees located on asphalt surfaces.

The proportions of different land use types in the four cases are summarised in Table 3. The percentages show that the study sites primarily consist of asphalt surfaces. Related to trees, the overall cross sectional areas of the tree crowns were considered for the analysis of shading effects on human thermal comfort. For the current land use configuration (case A), the selected NNE-SSW oriented street canyon has a higher proportion of grasslands and larger cross sectional areas of trees than the ESE-WNW oriented street canyon (Table 4).

**Table 4**  
Characteristics of the ESE-WNW and NNE-SSW street canyons within the simulation domain.

	ESE-WNW			NNE-SSW
	Total	SSW-facing sidewalk	NNE-facing sidewalk	Total
Length (m)	56	56	56	48
Width $W$ (m)	20	3	3	29
Horizontal area $A$ (m <sup>2</sup> )	1120	168	168	1392
Building height $H$ (m)	10.3	–	–	9.6
$H/W$	0.5	–	–	0.3
Contribution of asphalt surfaces to $A$ (%)	71	65	93	35
Contribution of grasslands to $A$ (%)	28	33	7	64
Contribution of overall cross sectional areas of the tree crowns to $A$ (%)	26	66	0	41

### 3. Results

#### 3.1. Validation of the ENVI-met simulation

To validate the human-biometeorological performance of the ENVI-met model, numerical simulations on 27 July 2009 were

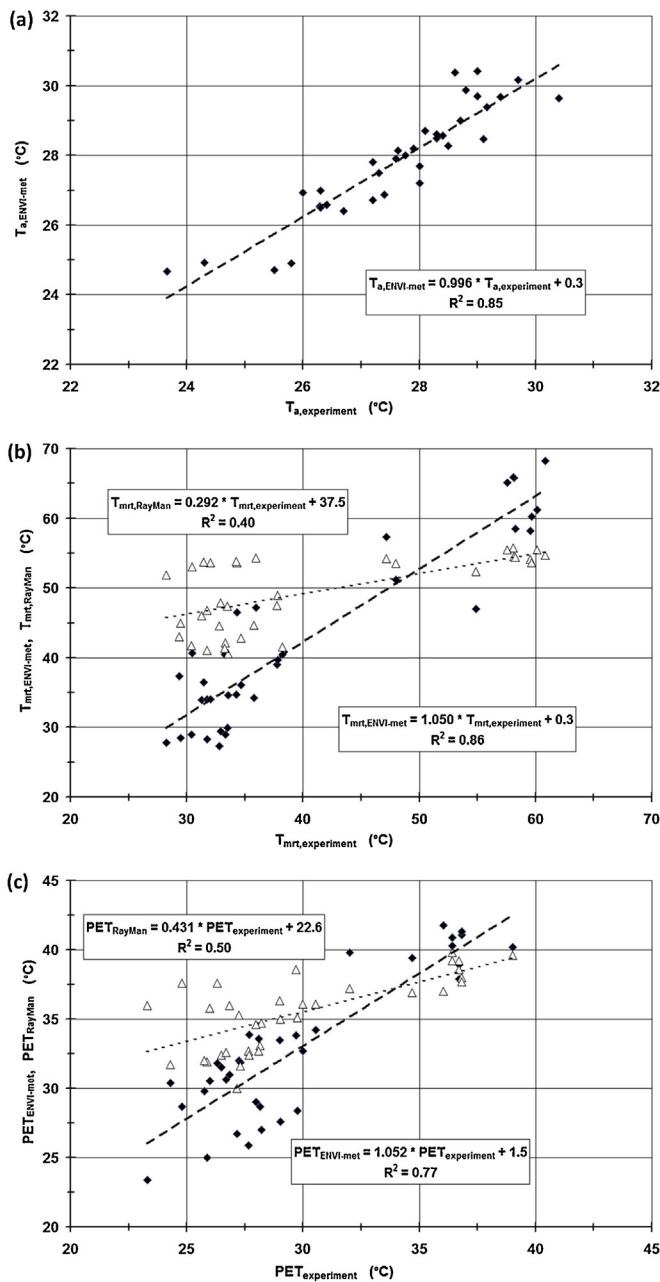


Fig. 3. Comparison between 1-h simulated and experimentally determined values of (a)  $T_a$ , (b)  $T_{mrt}$  and (c) PET (at a height of 1.5 m agl) on 29 July 2009 in the period 10-16 CET, simulation models ENVI-met and RayMan.

performed for case A (Fig. 2). The 1-h values of  $T_a$ ,  $T_{mrt}$  and PET at a height of 1.5 m agl were examined and the period between 10-16 CET was included. The validation of each variable was based on 35 pairs of simulated values and values determined by measurement data collected at five measuring sites.

The result shows that the ENVI-met model constantly overestimates  $T_a$  by approximately 0.2 K regardless of different  $T_a$  values (Fig. 3a). ENVI-met also overestimates  $T_{mrt}$  and PET, but the differences increase with increasing  $T_{mrt}$  and PET values (Fig. 3b and c). The differences in  $T_{mrt}$  between the simulation and measurement are 1.8 K for  $T_{mrt,experiment} = 30^\circ\text{C}$  and 3.3 K for  $T_{mrt,experiment} = 60^\circ\text{C}$ . The differences in PET are 2.8 K for  $PET_{experiment} = 25^\circ\text{C}$  and 3.6 K for  $PET_{experiment} = 40^\circ\text{C}$ .

The accuracy of the human-biometeorological performance of the ENVI-met version is examined using the difference measures

Table 5

Quantitative measures of the performance of the ENVI-met model and RayMan software package based on measured and experimentally determined  $T_a$ ,  $T_{mrt}$  and PET values at a height of 1.5 m agl (sample size: each 35);  $R^2$ : coefficient of determination, RMSE: root mean square error, RMSEs: systematic root mean square error, RMSEu: unsystematic root mean square error,  $d$ : Willmott's index of agreement.

	$R^2$	RMSE (K)	RMSEs (K)	RMSEu (K)	$d$
ENVI-met V4					
$T_a$	0.85	0.66	0.19	0.62	0.95
$T_{mrt}$	0.86	5.49	2.39	4.94	0.95
PET	0.77	3.98	3.06	2.52	0.84
RayMan Pro					
$T_{mrt}$	0.40	12.63	11.98	4.06	0.64
PET	0.50	6.40	6.13	1.89	0.60

of the model evaluation (Table 5), which have already been used by Yang et al. (2013): the coefficient of determination ( $R^2$ ), the root mean square error (RMSE), the systematic root mean square error (RMSEs), the unsystematic root mean square error (RMSEu) and Willmott's index of agreement ( $d$ ), which describes how error-free variables are simulated by a model. Simulation results are regarded as reliable if these measures are close to the following requirements: RMSEs  $\rightarrow$  0 K, RMSEu  $\rightarrow$  RMSE, and  $d \rightarrow$  1.0.

The  $R^2$  value indicates a strong correlation between simulated and experimentally determined  $T_{mrt}$  ( $R^2 = 0.86$ ) and  $T_a$  ( $R^2 = 0.85$ ). It is slightly lower for PET ( $R^2 = 0.77$ ). RMSE ranges from 0.66 K ( $T_a$ ) to 5.49 K ( $T_{mrt}$ ). RMSEs is relatively low for  $T_a$  (0.19 K), but higher for  $T_{mrt}$  (2.39 K) and PET (3.06 K). Related to RMSE, RMSEu amounts to 94% for  $T_a$ , 90% for  $T_{mrt}$  and 63% for PET. The  $d$  value ranges from 0.84 (for PET) to 0.95 (for  $T_a$  and  $T_{mrt}$ ). Based on the results in Table 5, the ENVI-met model V4 can provide reasonable predictions of  $T_a$ ,  $T_{mrt}$  and PET in a complex urban environment.

For comparison, 1-h values of  $T_{mrt}$  and PET from 10-16 CET were simulated at the sites mp1 through mp5 using the software package RayMan Pro V2.0. RayMan (Matzarakis, Rutz, & Mayer, 2010) is frequently applied worldwide to study human-biometeorological conditions at selected sites. Measured data including  $T_a$ ,  $v$ , and VP values at the five sites, as well as fish-eye photos showing the whole upper half space at each site, were used in the RayMan simulations. The results show that RayMan overestimates  $T_{mrt}$  by 16.3 K for  $T_{mrt,experiment} = 30^\circ\text{C}$  and underestimates  $T_{mrt}$  by 5.0 K for  $T_{mrt,experiment} = 60^\circ\text{C}$  (Fig. 3b). PET is overestimated by 8.4 K for  $PET_{experiment} = 25^\circ\text{C}$  and underestimated by 0.2 K for  $PET_{experiment} = 40^\circ\text{C}$  (Fig. 3c). Linear regressions between 1-h simulated and experimentally determined values were derived for  $T_{mrt}$  as well as PET. The regressions show relatively scattered patterns, especially for low values where the sites were covered in shading from tree canopies. Comparing the evaluation results of the performances of the two models (Table 5), ENVI-met V4 seems to be better suited than RayMan to simulate human thermal comfort in complex urban settings on hot summer days. The main reason may be the approach used in RayMan (Matzarakis et al., 2010) to determine the temperature of solid surfaces because its application is limited to relatively homogeneous conditions.

### 3.2. Simulation results

#### 3.2.1. Representation of the results

All simulation results refer to a height of 1.5 m agl, which approximates the human-biometeorological reference height of 1.1 m agl (Mayer, 1993). In the following the simulation results of  $T_a$ ,  $T_{mrt}$  and PET are presented in two ways: (i) spatial maps for the whole simulation domain (Figs. 4–12), and (ii) a table (Table 6) summarising the average values over

- the whole simulation domain,

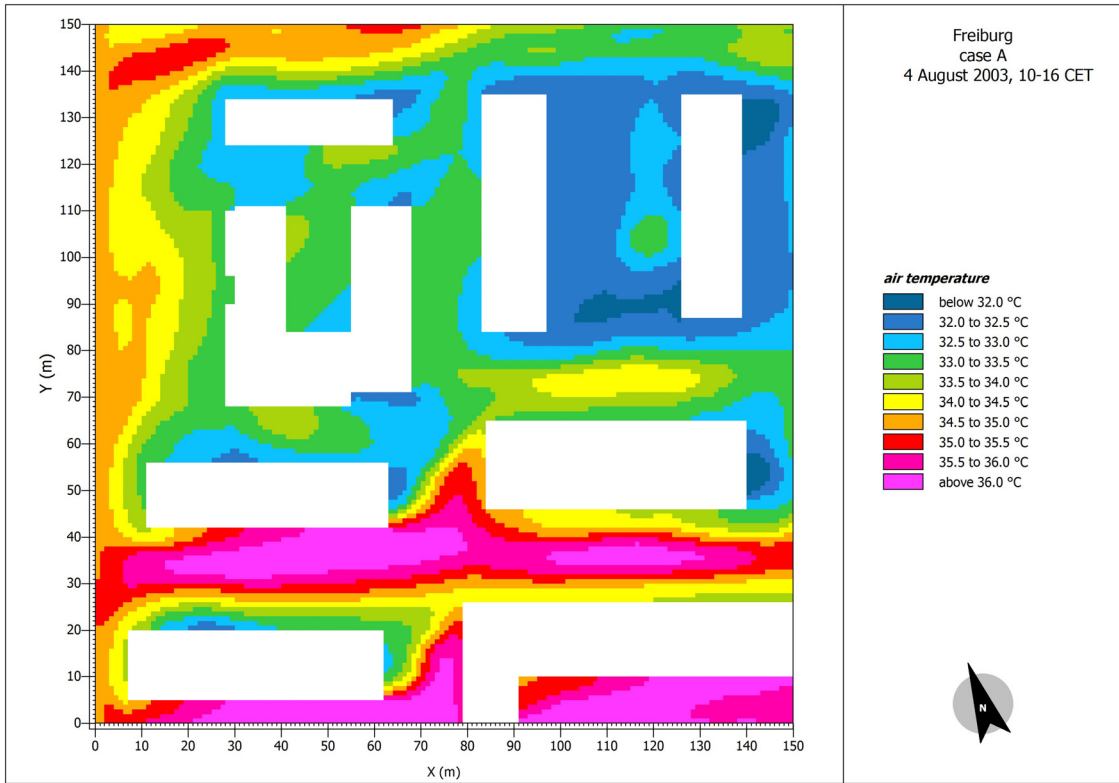


**Fig. 4.** Simulated  $T_a$  values at a height of 1.5 m agl for case A (current land use configuration) at a residential district in Freiburg averaged over 10-16 CET on the heat wave day of 4 August 2003 (white areas: buildings).

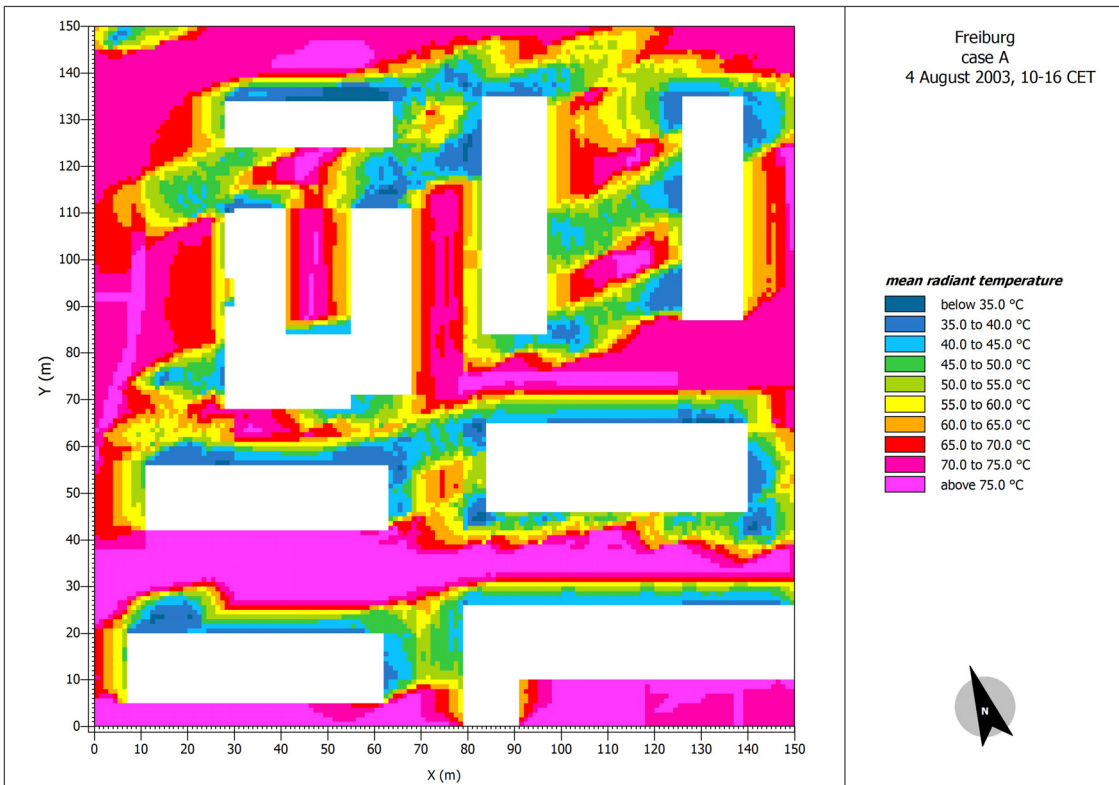


**Fig. 5.** Simulated  $T_{mrt}$  values at a height of 1.5 m agl for case A (current land use configuration) at a residential district in Freiburg averaged over 10-16 CET on the heat wave day of 4 August 2003 (white areas: buildings).

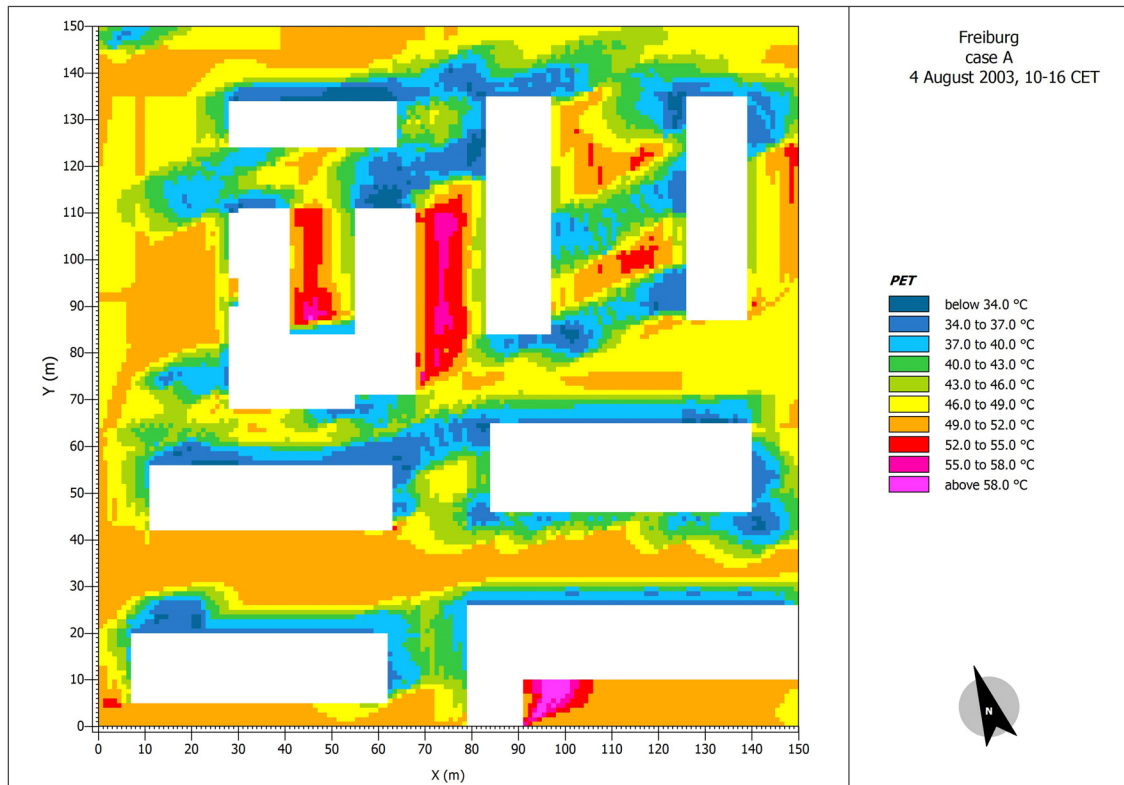


**Fig. 6.** Simulated PET values at a height of 1.5 m agl for case A (current land use configuration) at a residential district in Freiburg averaged over 10-16 CET on the heat wave day of 4 August 2003 (white areas: buildings).

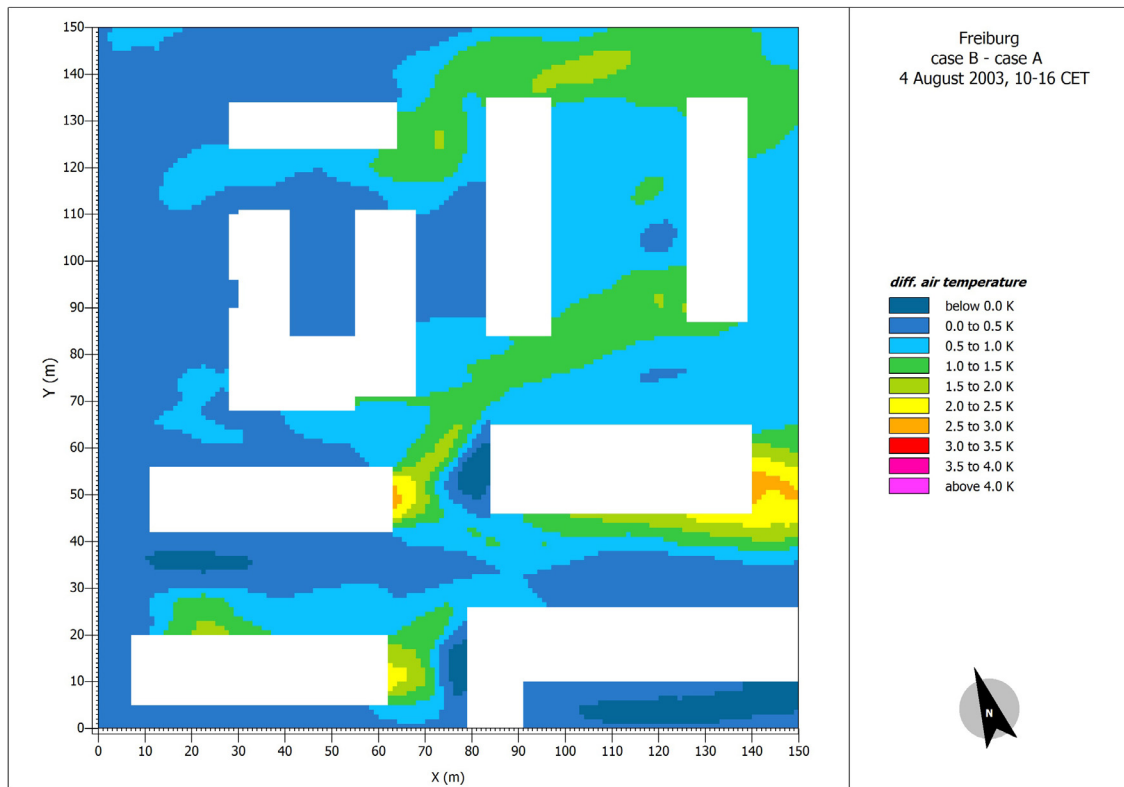


**Fig. 7.** Differences in simulated  $T_a$  values at a height of 1.5 m agl averaged over 10-16 CET between cases B and A (effect of trees on grasslands) at a residential district in Freiburg on the heat wave day of 4 August 2003 (white areas: buildings).

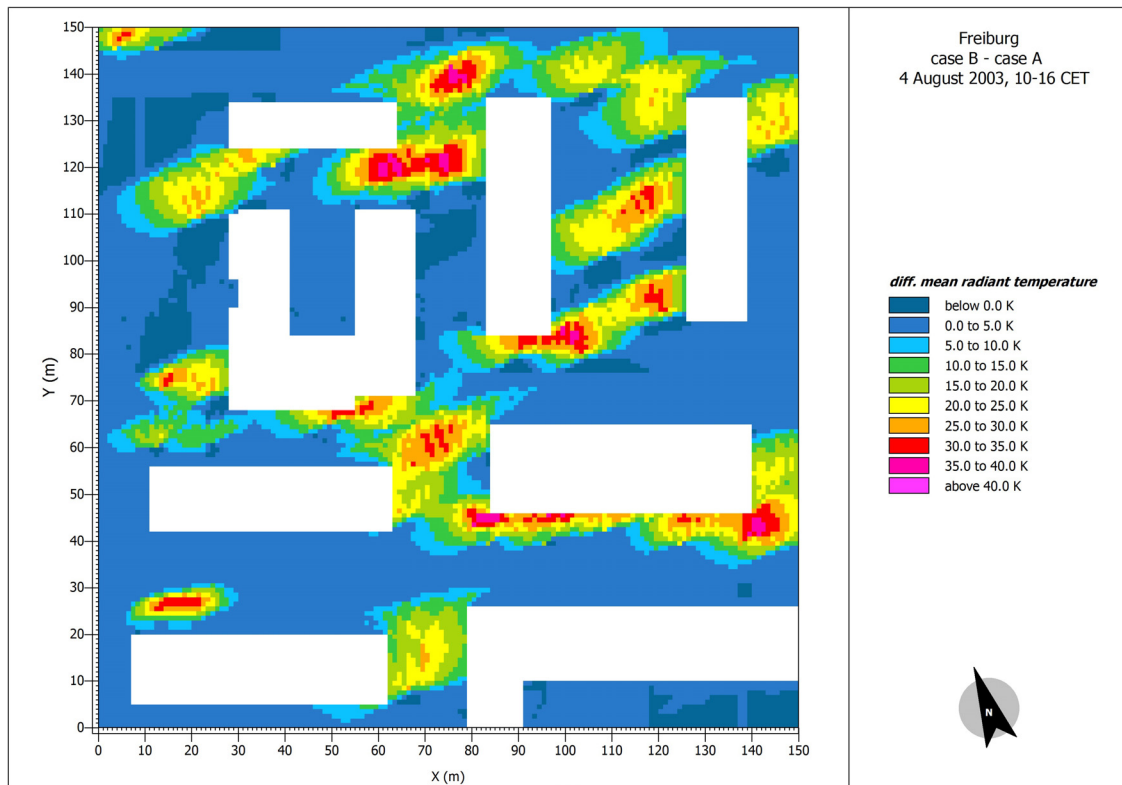


**Fig. 8.** Differences in simulated  $T_{mrt}$  values at a height of 1.5 m agl averaged over 10-16 CET between cases B and A (effect of trees on grasslands) at a residential district in Freiburg on the heat wave day of 4 August 2003 (white areas: buildings).

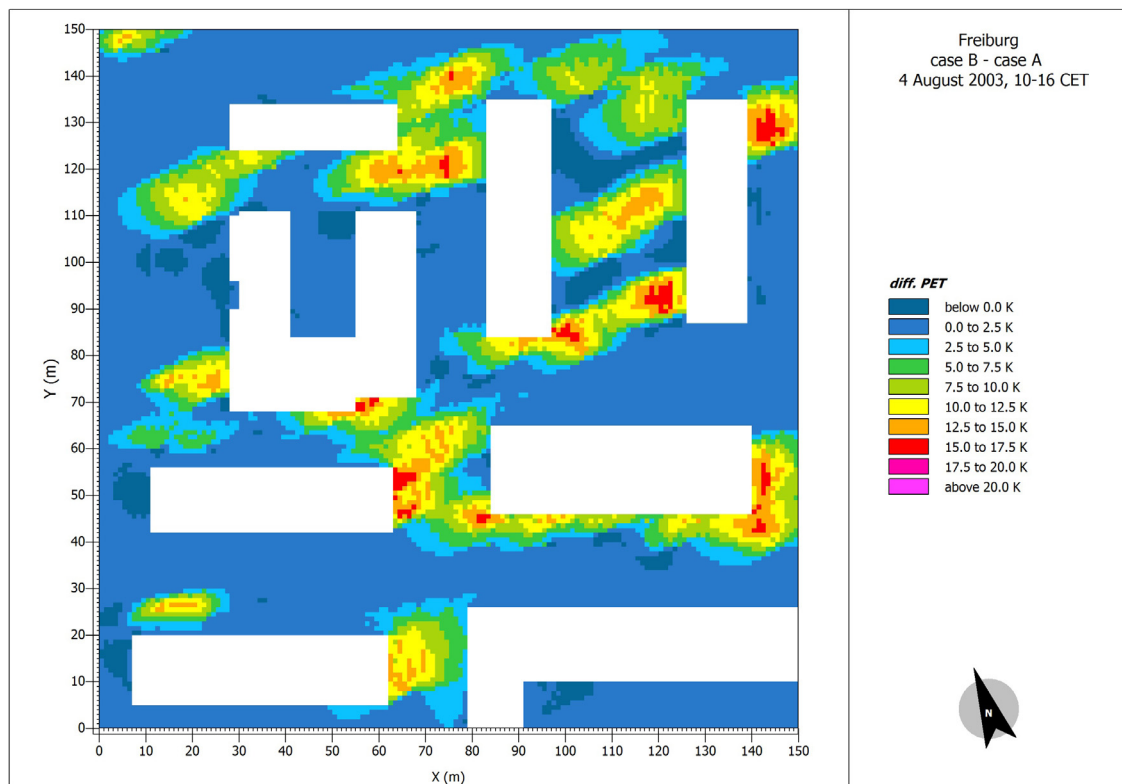


**Fig. 9.** Differences in simulated PET values at a height of 1.5 m agl averaged over 10-16 CET between cases B and A (effect of trees on grasslands) at a residential district in Freiburg on the heat wave day of 4 August 2003 (white areas: buildings).

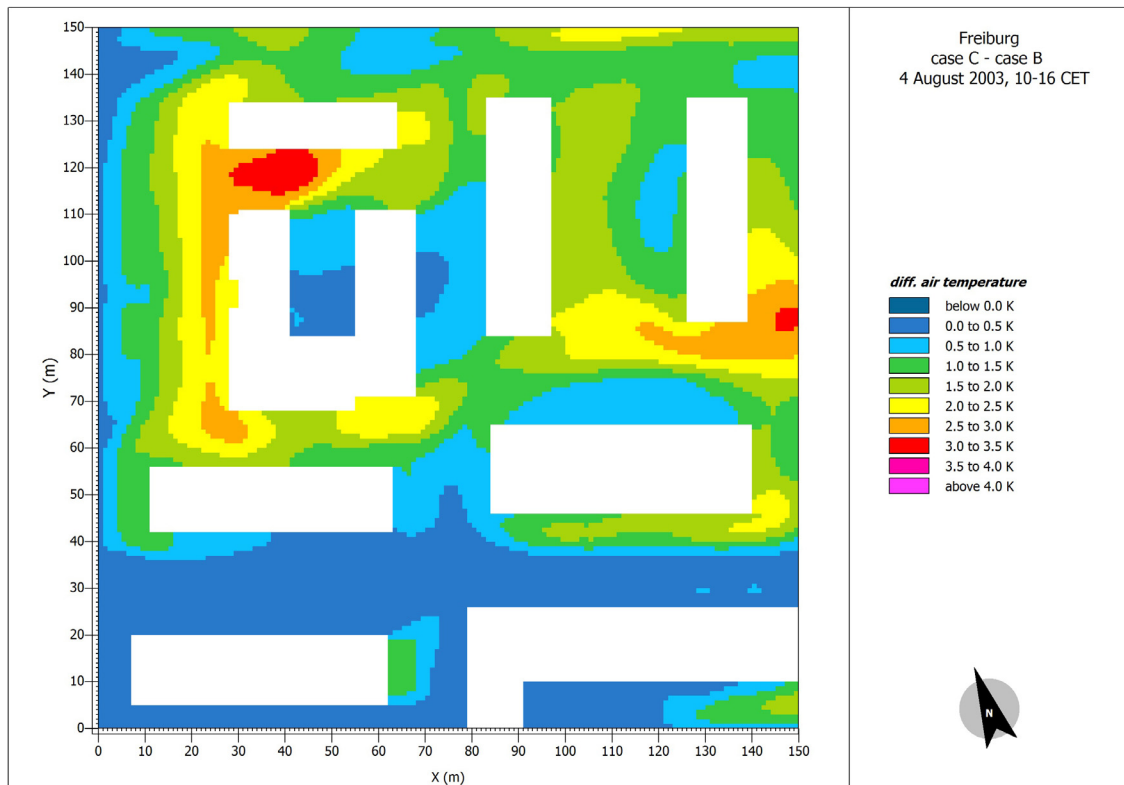


**Fig. 10.** Differences in simulated  $T_a$  values at a height of 1.5 m agl averaged over 10-16 CET between cases C and B (grassland effect) at a residential district in Freiburg on the heat wave day of 4 August 2003 (white areas: buildings).

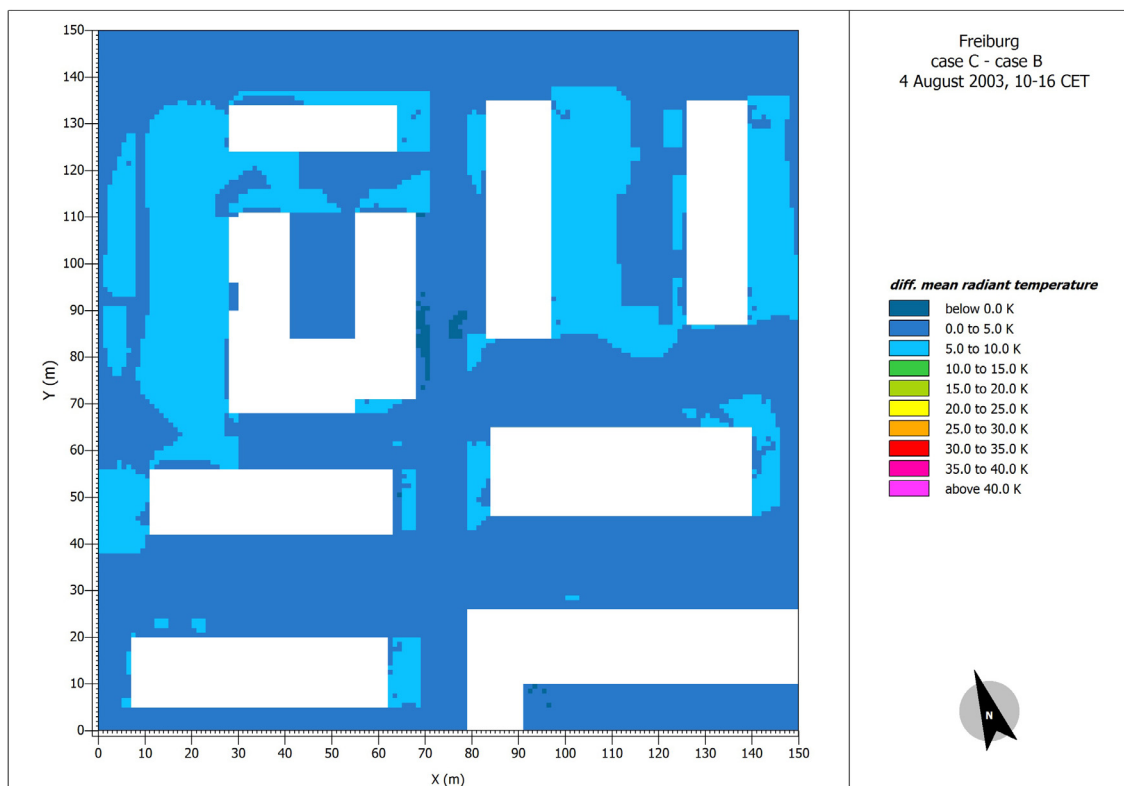


**Fig. 11.** Differences in simulated  $T_{mrt}$  values at a height of 1.5 m agl averaged over 10-16 CET between cases C and B (grassland effect) at a residential district in Freiburg on the heat wave day of 4 August 2003 (white areas: buildings).

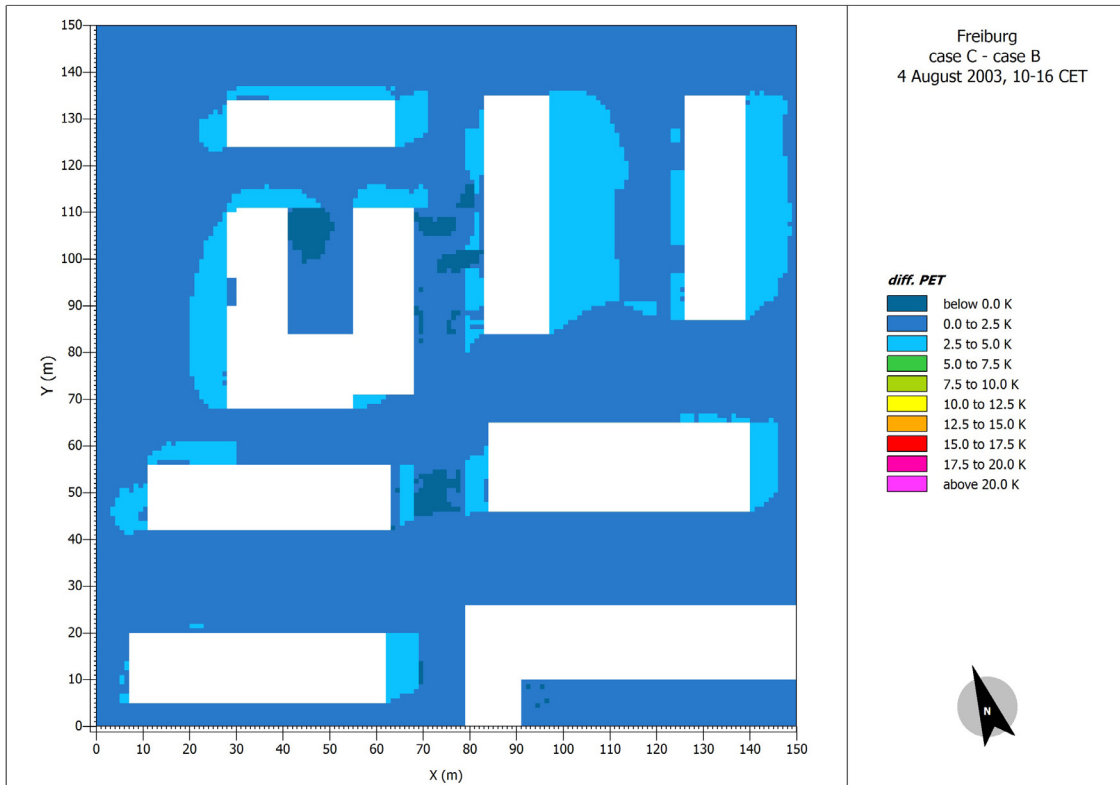


**Fig. 12.** Differences in simulated PET values at a height of 1.5 m agl averaged over 10-16 CET between cases C and B (grassland effect) at a residential district in Freiburg on the heat wave day of 4 August 2003 (white areas: buildings).

**Table 6**

Mean values of  $T_a$ ,  $T_{mrt}$  and PET (each in °C) at a height of 1.5 m agl for case A and the differences (each in K) between cases B and A (effect of trees on grasslands), C and B (grassland effect) as well as C and D (effect of trees on asphalt surfaces); different sections of the simulation domain in the periods of 10-16 CET and 22-05 CET for the heat wave day of 4 August 2003.

		10-16 CET				22-05 CET			
		A	B-A	C-B	C-D	A	B-A	C-B	C-D
Whole simulation domain	$T_a$	33.8	0.6	1.1	0.6	28.2	0.2	0.7	0.3
	$T_{mrt}$	61.8	6.6	2.4	6.1	21.8	-0.4	1.5	-0.2
	PET	45.3	3.0	1.0	2.6	24.1	0.0	1.1	0.2
ESE-WNW street canyon	$T_a$	34.9	0.7	0.7	0.7	28.7	0.1	0.4	0.2
	$T_{mrt}$	61.2	7.2	1.1	6.9	22.9	-0.5	0.9	-0.3
	PET	44.4	2.8	0.3	2.4	24.5	0.0	0.7	0.1
SSW-facing sidewalk	$T_a$	35.6	0.7	0.8	0.8	28.7	0.0	0.6	0.2
	$T_{mrt}$	71.1	4.9	1.2	4.9	22.9	-0.8	1.1	-0.4
	PET	47.8	2.0	0.2	1.8	24.5	-0.2	0.8	0.0
NNE-facing sidewalk	$T_a$	34.1	0.4	0.3	0.4	28.8	0.1	0.3	0.2
	$T_{mrt}$	42.8	0.3	0.4	0.3	23.3	-0.2	0.3	-0.1
	PET	37.5	0.5	0.4	0.5	24.8	0.1	0.3	0.2
NNE-SSW street canyon	$T_a$	32.3	0.8	1.4	1.0	28.5	0.5	0.7	0.7
	$T_{mrt}$	56.2	11.1	4.2	11.8	22.0	-0.8	2.1	-0.3
	PET	44.2	5.3	2.1	5.4	25.0	-0.2	1.4	0.2

- a section of an ESE-WNW oriented street canyon in the simulation domain (Fig. 2, case A),
- a section of a NNE-SSW oriented street canyon in the simulation domain (Fig. 2, case A),

- the SSW-facing sidewalk of the selected ESE-WNW oriented street canyon, and
- the NNE-facing sidewalk of the selected ESE-WNW oriented street canyon.

Figs. 4–12 were created using the LEONARDO software, which is included in ENVI-met. The base areas of the buildings are shown in a white colour, while the results of the simulated variables are shown in colour-coded ranges.

As the simulation results should be representative of outdoor summer heat environments for Central European citizens, they are averaged over the period from 10-16 CET (Holst & Mayer, 2011; Lee et al., 2014). To compare diurnal and nocturnal conditions on a heat wave day, Table 6 also lists  $T_a$ ,  $T_{mrt}$  and PET values averaged over the period from 22-05 CET. The spatial and temporal averaging of the simulation results over a longer simulation period can provide more pertinent urban design implications compared to single point investigations or short-term data such as 1-h simulation values.

### 3.2.2. Current land use configuration

For the current land use configuration (case A), Figs. 4–6 show the spatial variations for  $T_a$ ,  $T_{mrt}$  and PET, respectively. The spatial variations for  $T_{mrt}$  and PET are more significant than for  $T_a$ . The range for  $T_{mrt}$  is 33.1–79.4 °C, and the range for PET is 32.1–60.8 °C, compared to the range for  $T_a$ , which is from 31.5 to 36.7 °C. The intra-urban variability of  $T_a$  (~5 K) seems quite significant for a small site of 2.25 ha. However, this is reasonable in a complex urban environment with heterogeneous land surfaces and different geometries of buildings and trees, which cause various patterns of shaded and sunlit areas and also largely affect local ventilation.

With respect to  $T_a$ , the overall mean  $T_a$  in the diurnal period is 33.8 °C for case A (Table 6). For the two selected street sections, the diurnal mean  $T_a$  is 32.3 °C for the NNE-SSW oriented street canyon, which is significantly lower than that of the ESE-WNW oriented

street canyon, whose mean is 34.9 °C. The  $T_a$  difference between the two street canyons is caused not only by their different orientations but also by the higher overall cross sectional areas of tree crowns in the NNE-SSW street canyon. Spatial variation of  $T_a$  can also be observed within the same street canyon. For the two selected sidewalks within the ESE-WNW oriented street canyon, the mean  $T_a$  on the SSW-facing sidewalk is 35.6 °C, compared to the mean  $T_a$  on the NNE-facing sidewalk, which is 34.1 °C. The ~1.5 K difference in mean  $T_a$  reflects the impact of the local orientation to the sun on a heat wave day. For the nocturnal case, the overall mean  $T_a$  across the whole simulation domain is 28.2 °C, which is relatively high and can be considered to be a heat night. The highest nocturnal mean  $T_a$  (28.8 °C) occurs on the NNE-facing sidewalk.

$T_{mrt}$  shows more diverse spatial variations, which are caused by the pattern of shaded and sunlit areas (Fahmy & Sharples, 2009; Holst & Mayer, 2011; Lee et al., 2013; Lindberg & Grimmond, 2011; Shashua-Bar et al., 2011; Srivani & Hokao, 2013). The diurnal mean  $T_{mrt}$  is 61.8 °C for the whole simulation domain (Table 6). Similar to  $T_a$ , the mean  $T_{mrt}$  also shows significant differences for street canyons with different orientations. The diurnal mean  $T_{mrt}$  for the ESE-WNW oriented street canyon is 61.2 °C, which is significantly higher than that in the NNE-SSW oriented street canyon, which is 56.2 °C. The higher  $T_{mrt}$  can be attributed to the fewer number and smaller size of trees in the ESE-WNW street canyon. Within the same street canyon (ESE-WNW), the diurnal mean  $T_{mrt}$  for the NNE-facing sidewalk is 42.8 °C, whereas that for the SSW-facing sidewalk is 71.1 °C.

The diurnal mean PET value is 45.3 °C across the simulation domain (Table 6), which indicates hot thermal conditions for citizens according to the PET classification in Table 1. The diurnal mean PET in the ESE-WNW oriented street canyon is 44.4 °C, similar to that in the NNE-SSW oriented street canyon, which is 44.2 °C. Within the ESE-WNW oriented street canyon, the diurnal mean PET is 37.5 °C for the NNE-facing sidewalk, and 47.8 °C for the SSW-facing sidewalk. For the nocturnal case, the mean PET is 24.1 °C for the entire simulation domain, and is 24.5 °C and 25.0 °C for the ESE-WNW and NNE-SSW oriented street canyons, respectively. The difference between diurnal and nocturnal mean PET, which can be interpreted as thermo-physiologically significant cooling for citizens, is the highest (23.3 °C) at the SSW-facing sidewalk in the ESE-WNW oriented street canyon and the lowest (12.7 °C) at the NNE-facing sidewalk.

### 3.2.3. The effect of trees

The differences in the simulation results between cases B and A represent the human-biometeorological mitigation effect due to the shading of direct solar radiation by trees located on grasslands. The results (Table 6) show that the trees reduce the overall diurnal mean  $T_a$  by 0.6 K, mean  $T_{mrt}$  by 6.6 K, and mean PET by 3.0 K. Figs. 7–9 display the spatial variations of the differences in  $T_a$ ,  $T_{mrt}$  and PET between the two cases. They reveal that the mitigating effect of trees is up to 2.7 K for  $T_a$ , 39.1 K for  $T_{mrt}$  and 17.4 K for PET. The differences in  $T_{mrt}$  and PET show more diverse spatial variations than  $T_a$ , with the strongest mitigating effect occurring around the spots where trees were removed in case B. Notably, the pattern of PET is similar to that of  $T_{mrt}$  because PET is mostly governed by  $T_{mrt}$  in the daytime during dry and hot summer days (Holst & Mayer, 2011; Lee et al., 2014).

Among the different sections of the simulation domain, the NNE-SSW oriented street canyon shows the greatest mitigating effect because of the increased number of tree canopies. The reduction rate is 0.8 K for the diurnal mean  $T_a$ , 11.1 K for mean  $T_{mrt}$ , and 5.3 K for mean PET (Table 6). In contrast, in the ESE-WNW oriented street canyon, the reduction rate is only 0.7 K for diurnal mean  $T_a$ , 7.2 K for mean  $T_{mrt}$ , and 2.8 K for mean PET. In particular, the NNE-facing sidewalk in this street canyon has no trees, which results in the

lowest mitigating effect. It is only 0.4 K for  $T_a$ , 0.3 K for  $T_{mrt}$ , and 0.5 K for PET.

Compared to the daytime conditions, the mitigating effect of trees is significantly lower at night. The reduction rate is 0.2 K for the overall nocturnal mean  $T_a$  and -0.4 K for mean  $T_{mrt}$ . For PET, there is no substantial difference between the two cases. Notably, the effect of trees at night is negative for  $T_{mrt}$ . This is due to the specific radiant budget under the tree canopies at night. The largest effect occurs in the NNE-SSW oriented street canyon ( $T_{mrt} = -0.8$  K), which has dense tree canopies. As a result, the difference in PET is also negative, i.e., -0.2 K.

In addition to the differences between cases B and A, the differences in the simulation results between cases C and D reveal the impacts of trees located on asphalt surfaces instead of grasslands. The results are also summarised in Table 6. They are quite similar to the differences between cases B and A, with slightly higher changes in mean  $T_a$  such as the 0.2 K increase in the NNE-SSW oriented street canyon. This can be explained by the change to asphalt surfaces, which have lower albedo and emissivity compared to grasslands. On the other hand, the changes in  $T_{mrt}$  present a more scattered picture. While the diurnal mean  $T_{mrt}$  change in the ESE-WNW oriented street canyon is lower for trees on asphalt surfaces than trees on grasslands, i.e., 6.9 K vs. 7.2 K, it is higher in the NNE-SSW oriented street canyon, i.e., 11.8 K vs. 11.1 K. This inconsistency also reflects the complexity of surface radiation fluxes in complex urban environments.

### 3.2.4. The effect of grasslands

The differences in  $T_a$ ,  $T_{mrt}$  and PET between cases C and B, which represent the mitigating effect due to grasslands, are summarised in Table 6. The proportion of asphalt surfaces in the whole simulation domain increased from 41% in case B to 69% in case C. The results show that grasslands reduce the overall diurnal mean  $T_a$  by 1.1 K, mean  $T_{mrt}$  by 2.4 K, and mean PET by 1.0 K. Figs. 10–12 display the spatial variations of the differences in  $T_a$ ,  $T_{mrt}$  and PET between the two cases. They reveal that the mitigating effect of grasslands is up to 3.4 K for  $T_a$ , 7.5 K for  $T_{mrt}$  and 4.9 K for PET. It follows that the mitigating effect of grasslands on  $T_a$  is higher than that of trees. An exception is the NNE-facing sidewalk in the ESE-WNW oriented street canyon, which has almost no grass coverage.

The grassland effect on the diurnal mean  $T_{mrt}$  and PET is distinctly lower in all selected sections of the study site than the comparable effects of both tree versions (Table 6). For example, the mean  $T_{mrt}$  change in the whole simulation domain is 6.6 K for trees on grasslands and 6.1 K for trees on asphalt surfaces, respectively, while it amounts to only 2.4 K for grasslands. Among the selected sections, the mean  $T_{mrt}$  and PET changes due to grasslands are the highest (4.2 K for  $T_{mrt}$  and 2.1 K for PET) in the NNE-SSW street canyon, where the grass coverage is most pronounced.

In contrast to the daytime case, the cooling effect of grasslands at night (Table 6) is significantly higher than that of trees, resulting in larger decreases in  $T_a$ ,  $T_{mrt}$  and PET. For the whole simulation domain, mean changes due to grasslands are 0.7 K for  $T_a$ , 1.5 K for  $T_{mrt}$  and 1.1 K for PET. This could be attributed to the specific nocturnal radiant budget below tree canopies.

## 4. Discussion

### 4.1. Selection of suitable human-biometeorological simulation models

In this study, the up-to-date version V4 of the ENVI-met model was used. The human-biometeorological model performance in terms of simulating  $T_a$ ,  $T_{mrt}$  and PET was validated. Although a number of previous attempts have been made to validate the ENVI-met

model (Acero & Herranz-Pascual, 2015; Chen & Ng, 2013; Chow & Brazel, 2012; Chow, Pope, Martin, & Brazel, 2011; Jänicke, Meier, Hoelscher, & Scherer, 2015; Middel et al., 2014; Müller et al., 2014; Ng et al., 2012; Skelhorn et al., 2014; Srivani & Hokao, 2013; Yang et al., 2013), they mostly used early versions of ENVI-met and were focused only on  $T_a$ . Goldberg, Kurbjuhn, and Bernhofer (2013) have reported the physical drawbacks of previous versions of ENVI-met. In the current V4 version, such drawbacks have been eliminated, and regulating functions such as forcing with meteorological data have been added to control the simulation and increase accuracy. Over all, simulation results such as the  $T_a$  and  $T_{mrt}$  values agree much better with measurement data compared to studies using early versions of ENVI-met (Tan, Lau, & Ng, 2015). With high spatial resolution up to 0.5 m, the ENVI-met model V4 can simulate the micro-meteorological conditions in complex urban settings well and accurately evaluate outdoor human thermal comfort. The meteorological initialisation function of ENVI-met enables simulations of human thermal comfort for both current meteorological conditions in different climate zones and also future climate conditions as they are projected by regional climate models.

This study also used the RayMan software package in the validation process. In contrast to the ENVI-met model, RayMan was shown to be incapable of meeting the objective of this study, which is to model the micro-meteorological conditions in a heterogeneous urban micro-environment for urban design applications. Firstly, the validation results reveal that the  $T_{mrt}$  and PET conditions in complex urban micro-environments cannot be simulated accurately by RayMan Pro due to its limitations in dealing with large numbers of tree canopies. Secondly, RayMan can only investigate the micro-meteorological parameters at individual spots. Therefore, it is incapable of simulating spatial patterns of parameters such as  $T_{mrt}$  and PET. The visual as well as analytical representations of such parameters are important in urban design, as they can increase understanding of the cost-effect of different design strategies.

#### 4.2. Notes on scenario testing

The testing of different urban green scenarios presented in this study is particularly revealing to urban design practitioners, as it is related to a heat wave day, and can help urban designers to consider the potential of different types of urban greening for local mitigation of severe heat. For the severe thermal conditions of a heat wave day in Central Europe, the simulation results show the contributions of trees and grasslands to the mitigation of human heat stress in the simulation domain. In general, the spatial patterns of  $T_a$ ,  $T_{mrt}$  and PET are largely influenced by the number and dimension of trees and the coverage of grasslands, proving that urban greening is an effective method for mitigating the local heat stress. Previous studies have investigated beneficial human-biometeorological impacts of trees through field studies and numerical simulations (Ali-Toudert & Mayer, 2006, 2007; Chen & Ng, 2012; Holst & Mayer, 2011; Lee & Mayer, 2013; Lee et al., 2013, 2014; Mayer et al., 2008, 2009; Müller et al., 2014; Perini & Magliocco, 2014; Shahidan, Jones, Gwilliam, & Salleh, 2012; Shashua-Bar et al., 2011; Shashua-Bar, Tsiros, & Hoffman, 2012; Taleghani et al., 2015). The foci of these studies have mainly been given to  $T_a$  for individual spots. This study expands the existing knowledge of the local mitigation of severe heat stress due to urban greening by including results of  $T_{mrt}$  and PET. In contrast to the short simulation periods used in previous investigations, such as 1-h mean values, this study simulated both diurnal and nocturnal periods in a typical heat wave day. Compared to single-spot investigations, this study selected representative street canyons in the simulation domain with different green coverage, which helps us interpret the simulation results within specific urban contexts.

The four different urban green scenarios reveal the contributions of trees and grasslands to local cooling. The magnitude of the simulated spatial and temporal changes of  $T_a$ ,  $T_{mrt}$  and PET within the whole simulation domain varies largely depending on the local urban morphology, type of green coverage and time of day. Due to differences in energy budget schemes, the spatial variations of  $T_a$ ,  $T_{mrt}$  and PET are larger in the daytime than at night. In the daytime, the maximum cooling effect by grasslands in terms of  $T_a$  is 3.4 K, which is slightly lower than that of trees on asphalt surfaces, i.e., 3.6 K, but slightly higher than that of trees on grasslands, i.e., 2.7 K. The maximum reduction of  $T_{mrt}$  (7.5 K) and PET (4.9 K) by the grassland effect is distinctly lower than that of trees on grasslands ( $T_{mrt} = 39.1$  K, PET = 17.4 K) and trees on asphalt surfaces ( $T_{mrt} = 37.9$  K, PET = 21.0 K). In the daytime, the spatial variations of all three parameters within the whole simulation domain are less significant for grasslands than those for trees, which can be explained by the large amount of shading caused by trees.

The differences in the simulation results between cases C and A reveal the overall mitigation effect on human heat stress by the current green configuration. In the daytime, the mean cooling effect of the green coverage is 1.7 K for  $T_a$ , 9.0 K for  $T_{mrt}$  and 4.0 K for PET, with maximum magnitudes of up to 4.6 K for  $T_a$ , 43.1 K for  $T_{mrt}$  and 21.6 K for PET under the deep shadows of trees. This represents a substantial local mitigation of human heat stress. The two selected street canyons show the mitigation effects of urban morphology, the size of tree canopies, and grassland coverage, as well as street orientation with respect to the sun. Due to its relatively large tree canopies, the NNE-SSW oriented street canyon shows a larger cooling effect in the daytime, up to 2.2 K for  $T_a$ , 15.3 K for  $T_{mrt}$  and 7.4 K for PET. Comparing the results for both sidewalks of the ESE-WNW oriented street canyon, the SSW-facing sidewalk has higher mean values for the green coverage effect than the NNE-facing sidewalk amounting to 1.5 K for  $T_a$ , 6.1 K for  $T_{mrt}$  and 2.2 K for PET.

From the human-biometeorological perspective, the diurnal mean PET of 45.3 °C in the current urban green scenario (case A) indicates a “hot” human thermal sensation for Central European citizens according to Table 1. A thermal sensation of “warm” can be only achieved in shadowed street canyons, such as at the NNE-facing sidewalk of the ESE-WNW oriented street canyon.

#### 4.3. Urban design implications

The increasing heat stress in cities represents a challenge for sustainable urban design. The urban human-biometeorological perspective should be considered in the mitigation of heat stress. As  $T_a$  only indicates the sensible heat, the additional results of  $T_{mrt}$  and a thermo-physiologically significant assessment index such as PET are necessary to quantify human heat stress. Normally human heat stress can be mitigated by two measures: shading of the direct solar radiation and ventilation. While the near-surface airflow is important in coastal and tropical cities where the humidity is relatively high, the regional wind speed is relatively low on heat wave days in Central Europe. Therefore, shading of the direct solar radiation is considered the most effective mitigation strategy. Direct solar radiation can be locally shaded by buildings as well as galleries, tree canopies, awnings and sunshades (Lee & Mayer, 2013). From a human-biometeorological point of view, shading by tree canopies is most important (Lee et al., 2013; Mayer et al., 2009), particularly in urban open spaces and street canyons with lower aspect ratios.

As shown in this simulation study, the mitigation of human heat stress in the daytime by tree canopies is much more effective than that by grasslands. In practice, different influencing factors should be taken into account when implementing green schemes, such as the location of trees, dimension of tree canopies, geometry and orientation of streets, sun position, and also requests by citizens. For example, in this case study in a Central European city, human heat

stress in the daytime is most severe on the SSW-facing sidewalk of an ESE-WNW oriented street canyon. Mitigating the local human heat stress requires a certain number of trees with fully developed crowns located in certain spots. With the help of numerical simulation tools such as ENVI-met, different scenarios can be tested. Based on the simulation results, an optimised green scheme can be determined, and relevant design guidelines can be addressed.

## 5. Conclusions

This paper studies the potential of urban greening to mitigate human heat stress in a residential district in Freiburg, Southwest Germany. A human-biometeorological approach is taken which looks at the spatial and temporal change in  $T_{mrt}$  and PET in addition to  $T_a$ . The micro-meteorological simulation model ENVI-met V4 was validated and applied in this study. Four different urban green scenarios were tested to examine the cooling effect of trees and grasslands. The results showed that trees are more effective in mitigating human heat stress than just grasslands. In future work, both street canyons and open spaces should be considered. More urban green scenarios, with systematically altered coverage of trees and grasslands should also be included to provide an understanding of the cooling effect of different configurations of urban greening, which can be better used in design practice.

## Acknowledgements

The German-Israeli Foundation for Scientific Research and Development (GIF) has supported this research under grant no. 955-36.8/2007. The authors would especially like to thank (i) Dr. Jutta Holst for providing quality-checked results of field studies, which were used for the validation of the human-biometeorological performance of the ENVI-met model V4 and the RayMan software package, and (ii) Prof. Dr. Michael Bruse for advising on human-biometeorological simulation questions.

## References

- Acero, J. A., & Herranz-Pascual, K. (2015). A comparison of thermal comfort conditions in four urban spaces by means of measurements and modelling techniques. *Building and Environment*, 93, 245–257. <http://dx.doi.org/10.1016/j.buildenv.2015.06.028>
- Ali-Toudert, F., & Mayer, H. (2006). Numerical study on the effects of aspect ratio and orientation of an urban street canyon on outdoor thermal comfort in hot and dry climate. *Building and Environment*, 41(2), 94–108. <http://dx.doi.org/10.1016/j.buildenv.2005.01.013>
- Ali-Toudert, F., & Mayer, H. (2007). Effects of asymmetry, galleries, overhanging façades and vegetation on thermal comfort in urban street canyons. *Solar Energy*, 81(6), 742–754. <http://dx.doi.org/10.1016/j.solener.2006.10.007>
- Beniston, M. (2013). Exploring the behaviour of atmospheric temperatures under dry conditions in Europe: Evolution since the mid-20th century and projections for the end of the 21st century. *International Journal of Climatology*, 33(2), 457–462. <http://dx.doi.org/10.1002/joc.3436>
- Bowler, D. E., Buyung-Ali, L., Knight, T. M., & Pullin, A. S. (2010). Urban greening to cool towns and cities: A systematic review of the empirical evidence. *Landscape and Urban Planning*, 97(3), 147–155. <http://dx.doi.org/10.1016/j.landurbplan.2010.05.006>
- Bruse, M., & Fleer, H. (1998). Simulating surface-plant-air interactions inside urban environments with a three-dimensional numerical model. *Environmental Modelling and Software*, 13(3–4), 373–384. [http://dx.doi.org/10.1016/S1364-8152\(98\)00042-5](http://dx.doi.org/10.1016/S1364-8152(98)00042-5)
- Chen, L., & Ng, E. (2012). Outdoor thermal comfort and outdoor activities: A review of research in the past decade. *Cities*, 29(2), 118–125. <http://dx.doi.org/10.1016/j.cities.2011.08.006>
- Chen, L., & Ng, E. (2013). Simulation of the effect of downtown greenery on thermal comfort in subtropical climate using PET index: A case study in Hong Kong. *Architectural Science Review*, 56(4), 297–305. <http://dx.doi.org/10.1080/00038628.2012.684871>
- Chow, W. T. L., & Brazel, A. J. (2012). Assessing xeriscaping as a sustainable heat island mitigation approach for a desert city. *Building and Environment*, 47, 170–181. <http://dx.doi.org/10.1016/j.buildenv.2011.07.027>
- Chow, W. T. L., Pope, R. L., Martin, C. A., & Brazel, A. J. (2011). Observing and modelling the nocturnal park cool island of an arid city: Horizontal and vertical impacts. *Theoretical and Applied Climatology*, 103(1), 197–211. <http://dx.doi.org/10.1007/s00704-010-0293-8>
- Cohen, P., Potchter, O., & Matzarakis, A. (2012). Daily and seasonal climatic conditions of green urban open spaces in the Mediterranean climate and their impact on human comfort. *Building and Environment*, 51, 285–295. <http://dx.doi.org/10.1016/j.buildenv.2011.11.020>
- Coutts, A. M., White, E. C., Tapper, N. J., Beringer, J., & Livesley, S. J. (2015). Temperature and human thermal comfort effects of street trees across three contrasting street canyon environments. *Theoretical and Applied Climatology*. <http://dx.doi.org/10.1007/s00704-015-1409-y>
- Erell, E., Pearlmutter, D., Boneh, D., & Bar Kuti, P. (2014). Effect of high-albedo materials on pedestrian heat stress in urban street canyons. *Urban Climate*, 10(2), 367–386. <http://dx.doi.org/10.1016/j.uclim.2013.10.005>
- Fahmy, M., & Sharples, S. (2009). On the development of an urban passive thermal comfort system in Cairo, Egypt. *Building and Environment*, 44(9), 1907–1916. <http://dx.doi.org/10.1016/j.buildenv.2009.01.010>
- Federal Statistical Office of Germany. (2011). *Demographic change in Germany – issue 2011. Rep. no. 1. pp. 1–39.*
- Goldberg, V., Kurbjuhn, C., & Bernhofer, C. (2013). How relevant is urban planning for the thermal comfort of pedestrians? Numerical case studies in two districts of the city of Dresden (Saxony/Germany). *Meteorologische Zeitschrift*, 22(6), 739–751. <http://dx.doi.org/10.1127/0941-2948/2013/0463>
- Hajat, S., & Kosatky, T. (2010). Heat-related mortality: A review and exploration of heterogeneity. *Journal of Epidemiology & Community Health*, 64(9), 753–760. <http://dx.doi.org/10.1136/jech.2009.087999>
- Holst, J., & Mayer, H. (2010). Urban human-biometeorology: Investigations in Freiburg (Germany) on human thermal comfort. *Urban Climate News*, 38, 5–10.
- Holst, J., & Mayer, H. (2011). Impacts of street design parameters on human-biometeorological variables. *Meteorologische Zeitschrift*, 20(5), 541–552. <http://dx.doi.org/10.1127/0941-2948/2011/0254>
- Höppe, P. (1999). The physiological equivalent temperature – A universal index for the biometeorological assessment of the thermal environment. *International Journal of Biometeorology*, 43(2), 71–75. <http://dx.doi.org/10.1007/s004840050118>
- Huttner, S. (2012). *Further development and application of the 3D microclimate simulation ENVI-met. PhD thesis, Johannes Gutenberg University Mainz.*
- Jänicke, B., Meier, F., Hoelscher, M.-T., & Scherer, D. (2015). Evaluating the effects of façade greening on human bioclimate in a complex urban environment. *Advances in Meteorology*, 1–15. <http://dx.doi.org/10.1155/2015/747259>, article id 747259
- Klemm, W., Heusinkveld, B. G., Lenzholzer, S., & van Hove, B. (2015). Street greenery and its physical and psychological impact on outdoor thermal comfort. *Landscape and Urban Planning*, 138, 155–163. <http://dx.doi.org/10.1016/j.landurbplan.2015.02.009>
- Kuttler, W. (2010). Urban climate, Part I. *Gefahrstoffe – Reinhaltung der Luft*, 70(7/8), 329–340. <http://dx.doi.org/10.1007/100704-009-0240-8>
- Laschewski, G., & Jendritzky, G. (2002). Effects of the thermal environment on human health: An investigation of 30 years of daily mortality data from SW Germany. *Climate Research*, 21(1), 91–103.
- Lee, H., & Mayer, H. (2013). Urban human-biometeorology supports urban planning to handle the challenge by increasing severe heat. In *Proc. 29th International PLEA Conference* (pp. 1–6). Session I.3.
- Lee, H., & Mayer, H. (2015). Green coverage changes within an ESE-WNW street canyon as a planning measure to maintain human thermal comfort on a heat wave day. *Proc. 31st International PLEA Conference, PU*, 84, 1–8.
- Lee, H., Holst, J., & Mayer, H. (2013). Modification of human-biometeorologically significant radiant flux densities by shading as local method to mitigate heat stress in summer within urban street canyons. *Advances in Meteorology*, 1–13. <http://dx.doi.org/10.1155/2013/312572>, article id 312572
- Lee, H., Mayer, H., & Schindler, D. (2014). Importance of 3-D radiant flux densities for outdoor human thermal comfort on clear-sky summer days in Freiburg, Southwest Germany. *Meteorologische Zeitschrift*, 23(3), 315–330. <http://dx.doi.org/10.1127/0941-2948/2014/0536>
- Lindberg, F., & Grimmond, C. S. B. (2011). Nature of vegetation and building morphology characteristics across a city: Influence on shadow patterns and mean radiant temperatures in London. *Urban Ecosystems*, 14(4), 617–634. <http://dx.doi.org/10.1007/s11252-011-0184-5>
- Matzarakis, A., Rutz, F., & Mayer, H. (2010). Modelling radiation fluxes in simple and complex environments: Basics of the RayMan model. *International Journal of Biometeorology*, 54(2), 131–139. <http://dx.doi.org/10.1007/s00484-009-0261-0>
- Mayer, H. (1993). Urban bioclimatology. *Experientia*, 49(11), 957–963. <http://dx.doi.org/10.1007/BF02125642>
- Mayer, H., & Höppe, P. (1987). Thermal comfort of man in different urban environments. *Theoretical and Applied Climatology*, 38(1), 43–49. <http://dx.doi.org/10.1007/BF00866252>
- Mayer, H., Holst, J., Dostal, P., Imbery, F., & Schindler, D. (2008). Human thermal comfort in summer within an urban street canyon in Central Europe. *Meteorologische Zeitschrift*, 17(3), 241–250. <http://dx.doi.org/10.1127/0941-2948/2008/0285>
- Mayer, H., Kuppe, S., Holst, J., Imbery, F., & Matzarakis, A. (2009). pp. 211–219. *Human thermal comfort below the canopy of street trees on a typical Central European summer day. Reports of the Meteorological Institute* (Vol. 18) University of Freiburg (Germany).
- McGregor, G. R. (2011). Human biometeorology. *Progress in Physical Geography*, 36(1), 93–109. <http://dx.doi.org/10.1177/0309133311417942>

- Middel, A., Häb, K., Brazel, A. J., Martin, C. A., & Guhathakurta, S. (2014). Impact of urban form and design on mid-afternoon microclimate in Phoenix local climate zones. *Landscape and Urban Planning*, 122, 16–28. <http://dx.doi.org/10.1016/j.landurbplan.2013.11.004>
- Moonen, P., Defraeye, T., Dorer, V., Blocken, B., & Carmeliet, J. (2012). Urban physics: Effect of the micro-climate on comfort, health and energy demand. *Frontiers of Architectural Research*, 1(3), 197–228. <http://dx.doi.org/10.1016/j.foar.2012.05.002>
- Mullaney, J., Lucke, T., & Trueman, S. J. (2015). A review of benefits and challenges in growing street trees in paved urban environments. *Landscape and Urban Planning*, 134, 157–166. <http://dx.doi.org/10.1016/j.landurbplan.2014.10.013>
- Müller, N., Kuttler, W., & Barlag, A.-B. (2014). Counteracting urban climate change: Adaptation measures and their effect on thermal comfort. *Theoretical and Applied Climatology*, 115(1–2), 243–257. <http://dx.doi.org/10.1007/s00704-013-0890-4>
- Ng, E., Chen, L., Wang, Y., & Yuan, C. (2012). A study of the cooling effects of greening in a high-density city: An experience from Hong Kong. *Building and Environment*, 47, 256–271. <http://dx.doi.org/10.1016/j.buildenv.2011.07.014>
- Perini, K., & Magliocco, A. (2014). Effects of vegetation, urban density, building height, and atmospheric conditions on local temperatures and thermal comfort. *Urban Forestry & Urban Greening*, 13(3), 495–506. <http://dx.doi.org/10.1016/j.ufug.2014.03.003>
- Rebetez, M., Mayer, H., Dupont, O., Schindler, D., Gartner, K., Kropp, J. P., et al. (2006). Heat and drought 2003 in Europe: A climate synthesis. *Annals of Forest Science*, 63(6), 569–577. <http://dx.doi.org/10.1051/forest:2006043>
- Samaali, M., Courault, D., Bruse, M., Olioso, A., & Occelli, R. (2007). Analysis of a 3D boundary layer model at local scale: Validation on soybean surface radiative measurements. *Atmospheric Research*, 85, 183–198. <http://dx.doi.org/10.1016/j.atmosres.2006.12.005>
- Shahidan, M. F., Shariff, M. K. M., Jones, P., Salleh, E., & Abdullah, A. M. (2010). A comparison of *Mesua ferrea* L. and *Hura crepitans* L. for shade creation and radiation modification in improving thermal comfort. *Landscape and Urban Planning*, 97, 168–181. <http://dx.doi.org/10.1016/j.landurbplan.2010.05.008>
- Shahidan, M. F., Jones, P. J., Gwilliam, J., & Salleh, E. (2012). An evaluation of outdoor and building environment cooling achieved through combination modification of trees with ground materials. *Building and Environment*, 58, 245–257. <http://dx.doi.org/10.1016/j.buildenv.2012.07.012>
- Shashua-Bar, L., Pearlmutter, D., & Erell, E. (2011). The influence of trees and grass on outdoor thermal comfort in a hot-arid environment. *International Journal of Climatology*, 31(10), 1498–1506. <http://dx.doi.org/10.1002/joc.2177>
- Shashua-Bar, L., Tsiros, I. X., & Hoffman, M. (2012). Passive cooling design options to ameliorate thermal comfort in urban streets of a Mediterranean climate (Athens) under hot summer conditions. *Building and Environment*, 57, 110–119. <http://dx.doi.org/10.1016/j.buildenv.2012.04.019>
- Skelhorn, C., Lindley, S., & Levermore, G. (2014). The impact of vegetation types on air and surface temperatures in a temperate city: A fine scale assessment in Manchester, UK. *Landscape and Urban Planning*, 121, 129–140. <http://dx.doi.org/10.1016/j.landurbplan.2013.09.012>
- Srivanit, M., & Hokao, K. (2013). Evaluating the cooling effects of greening for improving the outdoor thermal environment at an institutional campus in the summer. *Building and Environment*, 66, 158–172. <http://dx.doi.org/10.1016/j.buildenv.2013.04.012>
- Stewart, I. D., & Oke, T. R. (2012). Local climate zones for urban temperature studies. *Bulletin of the American Meteorological Society*, 93(12), 1879–1900. <http://dx.doi.org/10.1175/BAMS-D-11-000191>
- Taleghani, M., Kleerekoper, L., Tenpierik, M., & van den Dobbelsteen, A. (2015). Outdoor thermal comfort within five different urban forms in the Netherlands. *Building and Environment*, 83, 65–78. <http://dx.doi.org/10.1016/j.buildenv.2014.03.014>
- Tan, Z., Lau, K. K.-L., & Ng, E. (2015). Urban tree design approaches for mitigating daytime heat island effects in a high-density urban environment. *Energy and Building*, <http://dx.doi.org/10.1016/j.enbuild.2015.06.031>
- Yang, X., Zhao, L., Bruse, M., & Meng, Q. (2013). Evaluation of a microclimate model for predicting the thermal behavior of different ground surfaces. *Building and Environment*, 60, 93–104. <http://dx.doi.org/10.1016/j.buildenv.2012.11.008>